HHS Public Access

Author manuscript

*Immunohorizons*. Author manuscript; available in PMC 2020 November 06.

Published in final edited form as:

*Immunohorizons*. ; 4(5): 245–258. doi:10.4049/immunohorizons.2000015.

# MKP-1 Modulates Mitochondrial Transcription Factors, Oxidative Phosphorylation, and Glycolysis

**Christian Bauerfeld**[*], **Harvinder Talwar**[†], **Kezhong Zhang**[‡], **Yusen Liu**[§], **Lobelia Samavati**[†,‡]

[*]Division of Critical Care, Department of Pediatrics, Wayne State University School of Medicine and Detroit Medical Center, Detroit, MI 48201

[†]Division of Pulmonary & Critical Care and Sleep Medicine, Department of Medicine, Wayne State University School of Medicine and Detroit Medical Center, Detroit, MI 48201

[‡]Center for Molecular Medicine and Genetics, Wayne State University School of Medicine, Detroit, MI 48201

[§]Center for Perinatal Research, The Abigail Wexner Research Institute at Nationwide Children's Hospital, Columbus, OH 43215

## Abstract

Sepsis is the leading cause of death in the world. Recent reports suggest that in response to sepsis, metabolism of macrophages switches from oxidative phosphorylation to aerobic glycolysis. MAPK phosphatase (MKP)–1 (also known as DUSP1) localized in the nucleus and preferentially dephosphorylates p38 and JNK. MKP-1 controls the expression of numerous inflammatory genes and transcription factors, thereby regulating innate and adaptive immunity. MKP-1–deficient animals exhibit aberrant metabolic responses following bacterial infections with a markedly increased mortality in response to sepsis. Because metabolic reprogramming modulates immune responses to TLR-4 activation, we investigated the effect of MKP-1 deficiency on mitochondrial electron transport chains involved in oxidative phosphorylation and transcription factors regulating mitochondrial biogenesis. Mitochondrial biogenesis is regulated by three nuclear-encoded proteins, including transcription factor A (TFAM), nuclear respiratory factors (NRF-1), and peroxisome proliferator–activated receptor $\gamma$ coactivator-1-$\alpha$ (PGC-1$\alpha$). We show that MKP-1–deficient mice/ macrophages exhibit, at baseline, higher expression of oxidative phosphorylation, TFAM, PGC-1$\alpha$, and NRF-1 associated with increased respiration and production of reactive oxygen species as compared with wild-type mice. Surprisingly, MKP-1–deficient mice/ macrophages responded to *Escherichia coli* sepsis or LPS with an impaired metabolic switch;



**Address correspondence and reprint requests to:** Dr. Lobelia Samavati, Division of Pulmonary & Critical Care and Sleep Medicine, Department of Medicine, Wayne State University School of Medicine, 3 Hudson, 3990 John R Street, Detroit, MI 48201. ay6003@wayne.edu.

C.B. and H.T. contributed to the study design, conducted the analysis, interpreted the data, and drafted the manuscript. K.Z. participated in data interpretation and preparation of the manuscript. Y.L. and L.S. designed the study and participated in all areas of the research, data analysis, and writing of the manuscript. All authors have read and approved the final manuscript.

DISCLOSURES

The authors have no financial conflicts of interest.

The gene expression data presented in this article have been submitted to the National Center for Biotechnology Information's Gene Expression Omnibus (https://www.ncbi.nlm.nih.gov/geo/) under accession number GSE122741.

despite enhanced glycolysis, a preserved mitochondrial function and biogenesis are exhibited. Furthermore, inhibition of p38 MAPK had no significant effect on TFAM and NRF-1 either in MKP-1–deficient macrophages or in wild-type macrophages. These findings support the conclusion that MKP-1 plays an important role in regulating proteins involved in glycolysis and oxidative phosphorylation and modulates expression of mitochondrial transcription factors.

## INTRODUCTION

Systemic inflammatory response, sepsis, septic shock, and multiorgan failure syndrome (MOFS) collectively affect more than 750,000 patients annually in the United States. Mortality due to this condition has been estimated between 30 and 50%, with an extensive annual healthcare cost (1). Irrespective of the etiology, subjects suffering from systemic inflammatory response/sepsis may subsequently develop MOFS, which is associated with a high mortality in adults and children worldwide (2, 3). In addition to supportive therapy such as early administration of antibiotics, there are no causal therapies for sepsis (4). Regardless of the site and mechanism of injury, the host responds to the insults with an elevation of circulating proinflammatory cytokines, leading to end organ damage and a shift toward a stress response with profound metabolic derangements. In sepsis, there is an impaired oxygen use leading to a shift from oxidative phosphorylation (OxPhos) toward glycolysis (5), resembling aerobic glycolysis described first in cancer cells by O. Warburg (6). Our group and others have shown that the switch to aerobic glycolysis is partly due to aberrant OxPhos machinery during sepsis (7–9).

MKP-1 dephosphorylates TXY motifs on MAPKs, thereby negatively regulating MAPKs that are involved in the synthesis of proinflammatory cytokines (10–12). Among investigators, it is well accepted that MKP-1 (DUSP1) preferentially dephosphorylates p38 and JNK, but it also can regulate ERK (10, 13–15). The MKP-1 gene is an immediate-early gene whose promoter region contains numerous consensus sequences, including hypoxia-inducible factor (HIF), cAMP response elements (CRE), and glucocorticoid response elements (GRE) (16, 17). MKP-1 controls the expression of numerous inflammatory genes and transcription factors (18, 19) and plays a significant role in the pathogenesis of inflammatory and metabolic diseases including sepsis, asthma, sarcoidosis, obesity, and type II diabetes (18, 20–22). MKP-$1^{-/-}$ mice maintain lean body weight and do not develop obesity (23, 24), but these mice are significantly more susceptible to sepsis and produce substantially higher inflammatory cytokines and succumb to earlier death despite appropriate antibiotic therapy (13, 14, 21). This picture of an augmented inflammatory response and lack of improvement in response to antibiotic treatment in MKP-1 knockout animal resembles what is often seen in septic patients, who develop MOFS and have poor prognosis.

Recently, we have shown that bone marrow–derived macrophages (BMDMs) from MKP-1–deficient mice exhibit higher expression of HIF-1$\alpha$ (25, 26). HIF-1$\alpha$ is an important transcription factor and plays a critical role in adaptation to low oxygen tension and it regulates the metabolic switch to aerobic glycolysis during inflammatory response after TLR activation (27–30). We found significantly higher HIF-1$\alpha$ (25, 26), HIF-2$\alpha$, and HIF-1β

expression in MKP-1$^{-/-}$ mice and BMDMs in normoxic culture condition. Based on our novel data and previous observations that MKP-1 deficiency is associated with enhanced production of cytokines including TNF-$\alpha$, IL-1β, IL-6, and IL-17 as well as increased reactive oxygen species (ROS) and higher susceptibility to sepsis with higher mortality, we investigated a possible role of MKP-1 on mitochondrial biogenesis and the OxPhos machinery. We hypothesized that MKP-1 plays an important role in the maintenance of inflammation (20, 31) through aberrant metabolic reprogramming and mitochondrial function in response to LPS. Specifically, we focused on the role of MKP-1 in the regulation of mitochondrial function in BMDMs in response to LPS. We found that BMDMs from MKP-1$^{-/-}$ at baseline express higher levels of the mitochondrial transcription factor A (TFAM), the peroxisome proliferator–activated receptor $\gamma$ coactivator-1-$\alpha$ (PGC-1$\alpha$), and the nuclear respiratory factors 1 (NRF-1). These three transcription factors regulate mitochondrial biogenesis, mitochondrial gene expression, and OxPhos (7, 32). The increased levels of these transcription factors were associated with abundance of proteins involved in OxPhos in MKP-1$^{-/-}$ at baseline. Wild-type (WT) and MKP-1–deficient BMDMs responded to LPS treatment with a significant upregulation of genes in genes related to glycolysis; this upregulation was much more profound in MKP-1 BMDMs. In contrast, WT mice/BMDMs responded to sepsis and LPS treatment with downregulation of OxPhos, followed by recovery of OxPhos. In contrast, MKP-1–deficient BMDMs responded to LPS with a sustained OxPhos and minimal decreased in mitochondrial transcription factors (TFAM, PGC-1$\alpha$, and NRF-1) in response to TLR4 activation. In this study, we show that MKP-1 deficiency leads a significant upregulation of glycolysis but a persistent mitochondrial activity including mitochondrial biogenesis, OxPhos, and ROS production after LPS stimulation.

## MATERIALS AND METHODS

### Chemicals and Abs

All chemicals were purchased from Sigma-Aldrich (St. Louis, MO) unless specified otherwise. LPS was purchased from InvivoGen (San Diego, CA). SB302580, specific p38 inhibitor was purchased from Sigma-Aldrich. SP600125, HRP-conjugated anti-mouse and anti-rabbit IgG secondary Abs were purchased from Cell Signaling Technology (Beverly, MA) and anti-goat IgG secondary Abs were purchased from Santa Cruz Biotechnology (Santa Cruz, CA). β-Actin Ab was purchased from Thermo Fisher Scientific (Waltham, MA). Abs against mitochondrial complexes, cytochrome *c* oxidase subunit I (COXI) and COXIV were purchased from MitoSciences (Eugene, OR). NRF-1, TFAM, pp38, and PGC-1$\alpha$ Abs were purchased from Santa Cruz Biotechnology. Superoxide dismutase (SOD)2 (manganese SOD [MnSOD]) Ab was purchased from Proteintech (Rosemont, IL). SOD1 Ab (copper-zinc SOD [Cu/ZnSOD]) was purchased from MilliporeSigma (Billerica, MA). Glucose transporter (Glut)1 Ab was purchased from Invitrogen (Carlsbad, CA).

### Mice and isolation of BMDMs

Animal studies were approved by the corresponding University Committee of the Columbus Children's Research Institute on Use and Care of Animals. BMDMs from mice were prepared as described previously (25, 33, 34). Briefly, femurs and tibias from 6- to 12-wkold

mice were dissected, and the bone marrow was flushed out. Macrophages were cultured with IMDM media supplemented with 30% L929 supernatant containing macrophage-stimulating factor, glutamine, sodium pyruvate, 10% heat-inactivated fetal FBS, and antibiotics for 5–7 d. BMDMs were replated at a density of $2 \times 10^6$ cells per well the day before the experiment.

### *Mouse model of* Escherichia coli *sepsis*

WT mice and the MKP-$1^{-/-}$ mice were infected with or without *E. coli* as previously described (35). Briefly, *E. coli* (O55:B5, ATCC 12014) purchased from American Type Culture Collection (Manassas, VA) was grown in Luria broth at 37°C for 18 h, washed three times with PBS, and suspended in PBS. *E. coli* was injected into the tail veins of mice at $2.5 \times 10^7$ CFU/g body weight. Infected mice were euthanized using by pentobarbital.

### Protein extraction and immunoblotting

Following treatments, the cells were harvested and washed twice with PBS. Radioimmunoprecipitation assay buffer containing a protease inhibitor and antiphosphatase mixture inhibitors II and III (Sigma Chemicals) was added for protein extraction. The protein concentration was measured using the bicinchoninic acid assay (Thermo Fisher Scientific, Sacramento, CA). Proteins (10–25 μg) were then mixed with equal amounts of 2× sample buffer (20% glycerol, 4% $NaDodSO_4$, 10% 2-βME, 0.05% bromophenol blue, and 1.25 M Tris-HCl [pH 6.8]). The proteins were fractionated on a 10% $NaDodSO_4$–polyacrylamide gel and transferred to polyvinylidene difluoride membrane using a semi-dry transfer cell (Bio-Rad Laboratories), which was run at 18 V for 1 h. The membranes were blocked for 1 h in 5% nonfat dry milk in TBST (0.1% Tween 20) and washed. The polyvinylidene difluoride membranes were incubated with the primary Ab overnight at 4°C. The blots were washed three times with TBST and incubated for 2 h with the HRP-conjugated secondary anti-IgG Ab (1/5000 in 5% nonfat dry milk in TBST) at room temperature. Following this incubation, the membranes were washed three times in TBST and incubated for 5 min with a chemiluminescent reagent (GE Healthcare) to visualize immunoreactive bands. Images were captured on HyBlot CL film (Denville Scientific,, Metuchen, NJ) using JPI automatic x-ray film processor model JP-33. OD analysis of signals was carried out using ImageJ software. Equal loading of blots was shown by total p38 and β-actin.

### Separation of cytoplasmic and nuclear fractions.

Cytoplasmic and nuclear fractions were separated as described previously (36). Briefly, after treatment, the cells were resuspended in a hypotonic buffer (10 mm HEPES [pH 7.9], 0.5% IGEPAL, 2 mm $MgCl_2$, 10 mm KCl, 0.1 mm EDTA, 0.5 mm PMSF, 1.0 μg/ml leupeptin, and 1.0 μg/ml aprotinin) and incubated on ice for 10 min. After centrifugation at 14,000 × *g* for 1 min at 4°C, the supernatant (cytoplasmic) and the pellets (nuclear fraction) were collected.

### Oxygen consumption rate and extracellular acidification rate measurements.

Oxygen consumption rate (OCR) and extracellular acidification rate (ECAR) were measured in adherent macrophages with a XF96 Extracellular Flux Analyzer (Seahorse Bioscience, Billerica, MA) as described previously (37). BMDMs obtained from WT and MKP-$1^{-/-}$ mice were seeded in 12 wells of a $XF^e$ 24- cell culture microplate (Seahorse Bioscience) at a density of $100 \times 10^3$ cells per well in 200 μl of media. The cells were stimulated with LPS (100 ng/ml). After 24 h at 37°C in 5% $CO_2$ incubator, XF assay medium was then added to the plate and incubated at 37°C for another hour in a non-$CO_2$ incubator. The plate was placed onto the calibrated $XF^e$ Extracellular Flux Analyzer (Seahorse Bioscience) for analysis. The OCR and ECAR were measured simultaneously to comprehensively profile the metabolic function of the cells. The measurement parameters were 3-min mix time, 2-min wait time, and 3-min measure time. The sensor cartridge for the $XF^e$ analyzer was hydrated with XF calibrant (pH 7) at 37° C on a $CO_2$ incubator 24 h before each experiment. The injection port A on the sensor cartridge was loaded with 1 μM oligomycin (complex V inhibitor), 1 μM FCCP was loaded to port B, and 1 μM rotenone/antimycin A (inhibitors of complex I and complex III) was loaded to port C (29).

### Mitochondrial ROS measurements.

BMDMs were stimulated with LPS (100 ng/ml). To measure ROS, cells were incubated with 5 μM of CM-H2DCFDA (Invitrogen) for cytosolic ROS (cROS) and 1 μM of MitoSOX (Invitrogen) for mitochondrial ROS (mROS) in the dark for 20 min at 37°C. BMDMs were washed three times in PBS, and immediately resuspended in live-cell imaging media (Invitrogen). CM-H2DCFDA Green fluorescence emission at 530 nm under 495 nm excitation was recorded using a Synergy microplate reader. MitoSOX Red fluorescence emission at 595 nm under 510 nm excitation was recorded using a microplate reader (7). Experiments were performed at least in triplicate. Data presented as relative fluorescence intensity of CM-H2DCFDA or MitoSOX fluorescence.

### Statistical analyses.

Statistical analyses were performed using SPSS software, version 25.0 (SPSS, Chicago, IL). One-way ANOVA test and post hoc repeated measure comparisons (least significant difference) were performed to identify differences between groups. For all analyses, two-tailed $p$ values $<0.05$ were considered significant.

## RESULTS

MKP-1 is not only a critical regulator of innate and adaptive immunity, but is also involved in a multitude of metabolic processes, including fatty acid metabolism and lipogenesis (18, 21, 24, 38, 39). Sepsis is associated with profound metabolic derangements. One hallmark of sepsis is an impaired oxygen use leading to a shift toward glycolysis (5). Our group and others have shown that the switch to aerobic glycolysis is partly due to aberrant OxPhos during sepsis (7–9). In a murine model of gram (−) sepsis, MKP-$1^{-/-}$ mice exhibit substantially enhanced inflammation and increased mortality (21, 35). We recently have shown that MKP-$1^{-/-}$ mice exhibit dysregulated fatty acid metabolism during gram negative sepsis (35). Given the fact that metabolic reprogramming plays an important part in the

response to sepsis (40, 41), we hypothesize that an aberrant metabolisms in MKP-1$^{-/-}$ mice/cells contributes, at least in part, to the observed hyperinflammation and higher mortality in sepsis in these mice/cells. To explore the role of MKP-1 deficiency on the metabolic adaptation in sepsis, we induced sepsis in WT and MKP-1–deficient mice as previously described (35). RNA sequencing was conducted using hepatic RNA extracts. We focused on gene expression of glycolytic and OxPhos pathways because of their importance in sepsis. Comparing the genes between WT and MKP-1$^{-/-}$ mice at baseline and in response to *E. coli* sepsis using differential expression analysis for sequence count and considering a false discovery rate of <1%, we identified large sets of genes involved in glycolysis (Fig. 1A) and OxPhos (Fig. 1B) that were differentially expressed. In response to sepsis, WT mice showed a clear shift of expression of genes involved in OxPhos toward genes involved in glycolysis. This switch, also known as Warburg-like effect, is one of the hallmarks in sepsis (6, 29). MKP-1$^{-/-}$ mice failed to downregulate genes related to OxPhos; instead, we observed a significant upregulation of genes involved in glycolysis. Similarly, in MKP-1$^{-/-}$ mice, we observed increased gene expression for several subunits of OxPhos complexes (Fig. 1B). These data suggest a maladaptive response to LPS challenge in MKP-1 deficiency.

## Mitochondrial transcription factors (NRF-1 and TFAM and PGC-1α) are highly expressed in MKP-1$^{-/-}$ BMDMs

To further assess the molecular basis for metabolic maladaptation in MKP-1 deficiency at the cellular level, we further delineated the effect of LPS on BMDMs derived from WT and MKP-1$^{-/-}$ mice. The mitochondrial transcription machinery is complex and regulated by several nuclear-encoded transcription factors. The TFAM is a nuclear-encoded protein that governs mitochondrial biogenesis and the expression of both mitochondrial and nuclear-encoded proteins (42, 43). TFAM plays an important role in activating transcription at the two major promoters of mitochondrial DNA, the light strand promoter and the heavy strand promoter 1. In addition, TFAM plays an important role in organizing mitochondrial DNA (44). PGC-1$\alpha$ and NRF-1 and −2 regulate gene expression involved in maintenance of OxPhos and expression of mitochondrial gene that integrate cellular functions with a wide range of metabolic demands (7, 45). NRF-1 regulates numerous genes involved in OxPhos machinery in response to oxidative stress and is a key player in the transcriptional cascade involved in regulating mitochondrial biogenesis (7, 32). PGC-1$\alpha$ functions as a cotranscriptional regulation factor and activates NRF-1, which, in turn, induces the expression of TFAM (45). For these reasons, we investigated the levels of NRF-1, TFAM, and PGC-1$\alpha$ and the effect of MKP-1 deficiency on these transcription factors (TFs) in WT and MKP-1$^{-/-}$ BMDMs in response to LPS challenge. BMDMs from WT and MKP-1$^{-/-}$ mice were cultured side by side and challenged with LPS for different time periods. Total cell lysates were subjected to immunoblotting using specific Abs against NRF-1 (Fig. 2A, 2B), TFAM (Fig. 2C, 2D), and PGC-1$\alpha$ (Fig. 2E, 2F). As shown at baseline, MKP-1–deficient BMDMs exhibited higher levels for all three TFs. In WT BMDMs, we observed a time-dependent increase in NRF-1 protein levels after LPS challenge (Fig. 2A, 2B). The effect of LPS on NRF-1 in WT BMDMs was in line of our previous report (7). In contrast, NRF-1 was highly expressed at baseline in MKP-1$^{-/-}$ BMDMs, but upon LPS stimulation, its expression decreased in a time-dependent manner (Fig. 2A, 2B). We have observed similar trends in TFAM and PGC-1$\alpha$ expression (Fig. 2C–F).

### MKP-1$^{-/-}$ BMDMs exhibit higher expression of mitochondrial transcription factors (TFAM, NRF-1, and PGC-1α) in the cytosolic and nuclear fractions

Next, we assessed the cytosolic and nuclear accumulation of mitochondrial transcription factors (TFAM, NRF-1, and PGC-1$\alpha$) at baseline and in response to LPS stimulation for 3 h in BMDMs from WT and MKP-1–deficient mice. BMDMs were cultured under same conditions and nuclear and cytosolic fractions were subjected to Western blot analysis. TFAM, NRF-1, and PGC-1$\alpha$ levels were significantly increased at baseline and in response to LPS both in the cytosolic and nuclear fractions of MKP-1$^{-/-}$ BMDMs compared with WT BMDMs (Fig. 3A). Fig. 3B–D show the densitometric values expressed as fold changes for TFAM, NRF-1, and PGC-1$\alpha$ in the cytosolic and nuclear fractions.

### Higher basal protein levels of OxPhos and aberrant response to LPS challenge

The formation of the cellular energy carrier ATP is the result of both anaerobic and aerobic processes. Anaerobic ATP generation is catalyzed by phosphoglycerate kinase and pyruvate kinase, and GTP is produced by succinyl CoA synthetase. Under normal physiologic conditions in mammals, ~95% of cellular energy is generated through the aerobic pathway (8). Because we have seen higher mitochondrial transcription factors in MKP-1$^{-/-}$ BMDMs as compared with WT cells, we hypothesize that MKP-1$^{-/-}$ BMDMs may exhibit higher OxPhos proteins. BMDMs from WT and MKP-1$^{-/-}$ mice were challenged with LPS for different time periods and protein extracts were used for immunoblotting and analysis for subunits of OxPhos complexes. As shown, the NDUFB6, which is the subunit B6 of NADH (ubiquinone oxidoreductase complex I) was significantly increased at baseline in MKP-1$^{-/-}$ BMDMs as compared with WT BMDMs. NADH is the key enzyme in cellular energy metabolism and provides ~40% of the proton-motive force that is used during mitochondrial ATP production (46). The complex I plays a major role in the production of ROS. In response to LPS challenge, MKP-1$^{-/-}$ BMDMs did not increase NDUFB6 protein levels (Fig. 4A, 4B). In contrast, we observed a lower expression with for NDUFB6 in WT BMDMs, which increased in response to LPS after 3h (Fig. 4A, 4B). *Complex II* is also called succinate ubiquinone oxidoreductase or, more commonly, *succinate dehydrogenase complex*; it is the key mitochondrial enzyme connecting the tricarboxylic acid cycle and the electron transport chain (ETC) (47). We assessed the levels of complex II–70 kDa Flp in cell lysates of WT and MKP-1$^{-/-}$ BMDMs. After normalization to β-actin, we observed an increased basal expression for complex II protein in MKP-1$^{-/-}$ BMDMs as compared with WT. Surprisingly, the expression of complex II protein in MKP-1$^{-/-}$ BMDMs was not affected after LPS challenge up to6h and then decreased significantly at 24 h (Fig. 4C, 4D). Similarly, complex III–50 kDa protein levels were significantly elevated at baseline in MKP-1$^{-/-}$ BMDMs. In response to LPS, complex III protein was induced at 6 h in WT BMDMs, whereas MKP-1$^{-/-}$ BMDMs showed a significant decrease in complex III protein as early as 1 h after LPS stimulation (Fig. 4E, 4F). Cytochrome *c* oxidase (complex IV) is the terminal enzyme of the ETC. COXI is the catalytic subunit and we have shown previously that inflammation, including TNF-$\alpha$ and LPS, negatively regulates its activity (7, 8). Surprisingly, we observed that MKP-1–deficient macrophages as compared with WT macrophages that exhibit significantly higher COXI expression at baseline (Fig. 4G, 4H). Consistent with our previous report (7), LPS challenge led to a time-dependent increase in COXI protein levels in WT macrophages. In contrast, MKP-1–deficient macrophages failed

to augment COXI protein expression in response to LPS challenge. Furthermore, MKP-1–deficient BMDMs showed a significant decrease of COXI after 24 h after LPS challenge (Fig. 4G, 4H).

## Increased ROS in MKP-1–deficient macrophages

The mitochondrial OxPhos process includes an ETC in which $O_2$ functions as the terminal electron acceptor and is reduced to water (8). As a byproduct of the OxPhos process, an estimated 1–2% of cellular $O_2$ is converted into superoxide anions. ROS, including superoxide, hydrogen peroxide ($H_2O_2$), and hydroxyl radicals, constantly cause damage to biological molecules, including DNA. LPS-induced ROS is involved in macrophage activation through enhancement of p38 and JNK MAPKs (21, 48). To determine the changes in cROS or mROS production, BMDMs from MKP-$1^{-/-}$ and WT mice were cultured for 1 and 24 h in the presence and absence of LPS. The results in Fig. 5A, 5B clearly show that both cROS and mROS production are significantly increased (2-fold) at the basal level in MKP-$1^{-/-}$ BMDMs. Interestingly, in response to 1 h LPS challenge, WT BMDMs enhanced both cROS and mROS (2-fold). In line with our previous observations (25), MKP-$1^{-/-}$ macrophages exhibited higher mROS and cROS production at baseline, which, in response to LPS, increased by 35% (Fig. 5A, 5B). As shown in Fig. 5C, 5D, 24 h after LPS challenge MKP-$1^{-/-}$ BMDMs did not significantly augment cROS and mROS production (~15%). In contrast, WT BMDMs responded to LPS challenge after 24 h with a modest increase (38%) in cROS and mROS (Fig. 5C, 5D).

## MKP-1–deficient BMDMs exhibit aberrant OCR and ECAR at baseline and in response LPS

OCR measures mitochondrial respiration, whereas ECAR is an indicator of glycolysis. To determine the effects of MKP-1 deficiency on OCR and ECAR, BMDMs obtained from WT and MKP-$1^{-/-}$ mice were cultured for 3 and 24 h in the absence and presence of LPS (100 ng/ml). Basal levels of OCR and ECAR are significantly increased in MKP-1–deficient BMDMs (Fig. 6A, 6B). Increased OCR and ECAR in MKP-$1^{-/-}$ macrophages indicate that both mitochondrial respiration and glycolysis are elevated at the baseline and in response to LPS. The results in Fig. 6A show that in the presence of LPS, OCR in WT BMDMs only minimally altered, whereas in MKP-$1^{-/-}$ BMDMs OCR is slightly reduced. In contrast, ECAR is elevated both in WT and MKP-$1^{-/-}$ macrophages after 3 h in response to LPS (Fig. 6B). Similarly, the results in Fig. 6C, 6D show that higher basal levels of OCR and ECAR in MKP-$1^{-/-}$ macrophages. After 24 h, LPS stimulation MKP-$1^{-/-}$ macrophages exhibited significantly higher ECAR but a reduced OCR, suggesting increased aerobic glycolysis. In the presence of LPS, the OCR is significantly reduced both in WT and MKP-$1^{-/-}$ macrophages (Fig. 6C), whereas ECAR is significantly increased both in WT and MKP-$1^{-/-}$ macrophages in response to LPS (Fig. 6D). The results demonstrate that MKP-1 deficiency enhances basal mitochondrial respiration and in response to LPS glycolysis is induced.

## Increased levels of SOD proteins and Glut1 in MKP-$1^{-/-}$ BMDMs

During mitochondrial respiration, electrons may leak during rapid electron flux and transferred to molecular oxygen to form superoxide anions. SODs are a class of antioxidant enzymes responsible for catalyzing of dismutation of superoxide anions ($O_2^-$) to form hydrogen peroxide ($H_2O_2$) (42). CuZnSOD (SOD1 protein) is a highly conserved enzyme

that is the primary cytoplasmic scavenger of superoxide radicals ($O_2^-$) (42, 43). MnSOD (SOD2 protein) is localized in the mitochondria, which produced more than 95% of superoxide radicals during OxPhos, and is the major antioxidant enzyme in the cells (49). Our group and others have shown that LPS challenge leads to rapid induction of SOD1 and 2 at the transcriptional and protein levels (7, 50, 51). This serves as a protective mechanism to prevent damage from excess ROS accumulation in the cell. To assess whether decreased SOD1 and/or SOD2 levels are responsible for the elevated ROS seen in MKP-$1^{-/-}$ macrophages, we cultured BMDMs of WT and MKP-$1^{-/-}$ in presence of absence of LPS for different time points. Total cell lysates were analyzed by immunoblotting using Abs for SOD1 and SOD2. MKP-$1^{-/-}$ BMDMs exhibit higher level of SOD1 as compared with WT BMDMs at baseline (Fig. 7A, 7B). Densitometric analysis of the ratio of SOD1/β-actin is shown in Fig. 7B. Interestingly, WT cells responded to LPS challenge with an enhanced SOD1 protein level. In contrast, we observed an abundance of SOD1 in MKP-$1^{-/-}$ BMDMs at baseline that did not further enhance upon LPS challenge. A similar pattern was observed for SOD2 (Fig. 7C, 7D). Additionally, WT BMDMs show increased levels of SOD1 and SOD2 in response to LPS, whereas MKP-$1^{-/-}$ BMDMs fail to show such upregulation. These data collectively indicate that increased ROS measurement in MKP-$1^{-/-}$ BMDMs is not due to lack of SODs.

GLUT1 facilitates the transports of glucose and ascorbic acid across the cell and mitochondrial membranes; it has been shown that in response to TLR activation, the expression of GLUT1 at the gene (*SLC2A1*) and protein levels increases. Because GLUT1 plays a critical role in glucose uptake in macrophages and derives the enhanced glycolysis during sepsis, we evaluated GULT1 expression in WT and MKP-$1^{-/-}$ BMDMs in response to LPS. As shown in Fig. 7E, 7F, GLUT1 in WT BMDMs was less abundant at baseline, LPS challenge led to rapid induction of GLUT1. In contrast, MKP-$1^{-/-}$ BMDMs exhibited higher level of GLUT1 protein, but LPS challenge did not further augment expression of GLUT1.

## Inhibition of p38 phosphorylation has no effect on LPS-induced mitochondrial transcription factors (NRF-1 and TFAM) expression

Next, we tested the effects of a specific p38 inhibitor (SB203580) on NRF-1 and TFAM protein expression in response to LPS. BMDMs derived from WT and MKP-$1^{-/-}$ mice were treated with SB203580 (10 μM) for 30 min prior to LPS stimulation for 3 h. Whole protein lysates were immunoblotted with specific Abs against pp38 ($Thr^{180}/Tyr^{182}$), NRF-1, and TFAM. As shown in Fig. 8A, LPS-mediated p38 phosphorylation was completely inhibited in the presence of SB203580 in both WT and MKP-$1^{-/-}$ BMDMs. In contrast, SB203580 had no effect on LPS-modulated NRF-1 and TFAM expressions (Fig. 8C, 8E). Densitometric analysis for pp38, NRF-1, and TFAM are shown in Fig. 8B, 8D, and 8F, respectively. Because MKP-1 also has been to modulate JNK activity, we also evaluated the effect of a JNK inhibitor on TFAM and NRF-1. When we used a specific inhibitor for JNK, we observed similar results as using p38 inhibitor (data not shown). These data suggest that neither p38 or JNK inhibition cannot abrogate the effect of MKP-1 deficiency on higher expression of TFAM and NRF-1.

## DISCUSSION

Sepsis is associated with a profound derangement of metabolism, including enhanced aerobic glycolysis with simultaneous suppression of OxPhos. The exact molecular mechanisms of this metabolic switch, also termed Warburg-like effect, during sepsis is poorly understood (52). It has been suggested that this metabolic switch associated with the severity of lactic acidosis may contribute to organ failure and mortality (53). The majority of shock-related deaths occur during this phase, likely because of bioenergetics failure, immune hyperresponsiveness, or the failure to contain the bacterial infection despite antibiotic treatment (7, 29, 54). Recent work suggests that immune hyperresponsiveness and mitochondrial dysfunction plays a central role in sepsis (55, 56). We have shown that septic MKP-1–deficient mice exhibit immune hyperresponsiveness but defective bacterial clearance and aberrant fatty acid metabolism (21, 35).

Our current data show that MKP-$1^{-/-}$ BMDMs have higher basal oxygen consumption and ECARs and produced more ROS than WT BMDMs. Among the transcriptional regulators, NRF-1 and TFAM govern mitochondrial gene expression, especially genes involved in OxPhos (7). NRF-1 and TFAM both showed higher expression in MKP-1–deficient macrophages. Furthermore, we discovered that mitochondrial TFs including, TFAM, NRF-1, and PGC-1$\alpha$ are robustly upregulated in MKP-$1^{-/-}$ BMDMs at baseline. Similarly, we observed higher levels of ETC (complex I–IV) proteins. In contrast, WT macrophages exhibited lower expression of mitochondrial transcription factors (TFAM, NRF-1, and PGC-1$\alpha$) along with lower ETC proteins. Similar to our previous report (7), we observed that levels of these proteins reversed in response to LPS challenge: WT macrophages increased expression for complex I (NDUFB6), complex III, and COXI after 6 h LPS treatment. Whereas MKP-$1^{-/-}$ BMDMs responded with a decreased expression of these proteins. Similarly, *E.coli* induced sepsis in WT mice led to clear upregulation of genes related to glycolytic pathways and downregulation of genes related to OxPhos (Fig. 1). In contrast, MKP-1–deficient mice failed to respond to sepsis with an incomplete metabolic switch. These genes also failed to tone down their expression in MKP-1 knockout mice following infection. Similar patterns were observed in MKP-$1^{-/-}$ BMDMs. Interestingly, pretreatment of macrophages with p38 inhibitor (SB 203580) did not affected expression of both transcription factors in neither WT nor MKP-1–deficient macrophages at baseline and in response to LPS, suggesting that abundance of NRF-1 and TFAM may not be due to increased p38 activation. Similarly, inhibition of JNK did not grossly change the expression of NRF-1 and TFAM in response to LPS (data not shown). Several investigators underlined the role of MKP-1 in metabolism even in the absences of sepsis (57). For instance, it has been shown that MKP-$1^{-/-}$ mice are resistant to age- and high-fat diet–induced obesity and do not develop fatty liver (37). Our results support the notion that MKP-1–deficient mice/macrophages have a higher metabolic rate with an increase in respiration, higher OxPhos, and increased ROS production. SOD1 and −2 are detoxifying enzymes located in the outer and inner mitochondrial membrane, respectively. SODs catalyze the dismutation of the superoxide ($O_2^-$) radicals into $H_2O_2$. In response to higher ROS production or LPS stimulation, SODs are rapidly induced to regulate dismutation of enhanced superoxide

production (52). Our data suggest that the increased ROS in MKP-1$^{-/-}$ BMDMs was not due to lack of scavenger enzymes, as SOD1 and 2 were highly expressed.

It has been shown that in response to endotoxemia the glucose uptake is rapidly augmented and increased expression of GLUT1 (SLC2A1) is the GLUT in macrophages (29, 53). Upon glucose uptake through the GLUT1 transporter, glucose is converted into pyruvate through a series of enzymatic reactions to generate pyruvate and two ATPs. Our current data show a significant higher expression of GLUT1 under basal conditions in MKP-1$^{-/-}$ macrophages, which only moderately increases in response to LPS challenge. During endotoxemia a metabolic switch from OxPhos to glycolysis occurs. This process is coordinated by a complex transcriptional program in which HIF-1$\alpha$ plays a central role (29, 34). Recently, we have shown that under normoxic conditions MKP-1$^{-/-}$ macrophages exhibit higher HIF-1$\alpha$ expression and activity (26), increased ROS and cytokine production and an increased OxPhos capacity. This was accompanied by increased protein levels and function of mitochondrial transcription factors including TFAM and NRF-1 (7, 58). MKP-1$^{-/-}$ mice/cells have preserved OxPhos and increased β-oxidation but also exhibit increased anaerobic glycolysis. In contrast, in response to sepsis, WT mice showed severely decreased expression of genes involved in OxPhos and upregulation of genes involved in glycolysis, known as Warburg effect. Furthermore, we have recently shown that in response to sepsis MKP-1$^{-/-}$ mice exhibit markedly disrupted lipid metabolism (35). In addition to enhanced GLUT1 expression in MKP-1$^{-/-}$ mice/cells, we identified enhanced expression of several key enzymes shown to be important in sepsis mediated glycolysis. We identified that hexokinase isoforms are highly upregulated in MKP-1. Similarly, we observed increased expression of several key enzymes in the glycolysis pathway, including, pyruvate kinase (PKM), phosphofructokinase (PFK), and aldehyde dehydrogenase (ALDH1A3 and ALDH3A1). Several of these enzymes are under the transcriptional regulation of HIF-1$\alpha$ (54, 55). These data suggest that lack of MKP-1 changes the transcriptional landscape related to glycolysis. The regulation and contribution of these key enzymes need further investigation. Given the fact that MKP-1$^{-/-}$ mice exhibit markedly increased mortality associated with septic shock (13, 14, 21), we propose that disrupted metabolic pathways may play a major role in the poor outcome of these mice. In this study, we show that MKP-1–deficient mice/macrophages have defects in adaptive metabolism in response to bacterial sepsis or LPS. In response to sepsis the MKP-1 deficient mice are unable to downregulate OxPhos despite augmented glycolysis. Previously, we have shown that in a murine model of gram (−) sepsis, MKP-1$^{-/-}$ mice exhibit substantially enhanced inflammation, aberrant metabolism, increased mortality, and decreased bacterial clearance (14, 21, 35). Recently, it has been shown that the changes in metabolism toward aerobic glycolysis are important step in macrophage function and the clearance of bacteria (29, 56, 57). Alternative explanations for decreased bacterial clearance in MKP-1$^{-/-}$ mice might be a relatively preserved OxPhos.

Our work provides a new layer to the complexity of the MKP-1 role in innate, adaptive, and metabolism. MKP-1 is a crucial gatekeeper of the innate immune response, which centered to its negative regulatory role as phosphatase (18). Because of its critical role of the innate immune response in the development of the adaptive immunity, it is not surprising that the MKP-1 has a profound impact on shaping adoptive immune responses (38). However, the

role of MPK-1 in metabolism and mitochondrial function appears to be more complex and multifaceted (22, 58). It has been shown that MKP-1 knockout mice/cells show lean body weight and resistance to high-fat diet–induced obesity. Similarly, our current data corroborate with these data showing enhanced OxPhos and ROS production and increased GULT1 expression. How MKP-1 regulates mitochondrial transcription factors and the OxPhos deserves further investigation.

## Acknowledgments

This work was supported by the Children's Hospital of Michigan Foundation (to C.B.) and by the following grants: R01HL113508 (to L.S.), and R01 AI124029 and R21 AI142885 (to Y.L.).

## Abbreviations used in this article:

| | |
|---|---|
| **BMDM** | bone marrow–derived macrophage |
| **COXI** | cytochrome *c* oxidase subunit I |
| **cROS** | cytosolic ROS |
| **ECAR** | extracellular acidification rate |
| **ETC** | electron transport chain |
| **Glut** | glucose transporter |
| **HIF** | hypoxia-inducible factor |
| **MOFS** | multiorgan failure syndrome |
| **mROS** | mitochondrial ROS |
| **NRF-1** | nuclear respiratory factor 1 |
| **OCR** | oxygen consumption rate |
| **PGC-1α** | peroxisome proliferator–activated receptor γ coactivator-1-α |
| **ROS** | reactive oxygen species |
| **SOD** | superoxide dismutase |
| **TF** | transcription factor |
| **TFAM** | mitochondrial transcription factor A |
| **WT** | wild-type |

## REFERENCES

1. Arefian H, Heublein S, Scherag A, Brunkhorst FM, Younis MZ, Moerer O, Fischer D, and Hartmann M. 2017 Hospital-related cost of sepsis: a systematic review. J. Infect. 74: 107–117. [PubMed: 27884733]

2. Randolph AG, and McCulloh RJ. 2014 Pediatric sepsis: important considerations for diagnosing and managing severe infections in infants, children, and adolescents. Virulence 5: 179–189. [PubMed: 24225404]

3. Brealey D, Karyampudi S, Jacques TS, Novelli M, Stidwill R, Taylor V, Smolenski RT, and Singer M. 2004 Mitochondrial dysfunction in a long-term rodent model of sepsis and organ failure. Am. J. Physiol. Regul. Integr. Comp. Physiol. 286: R491–R497. [PubMed: 14604843]

4. Nguyen HB, Jaehne AK, Jayaprakash N, Semler MW, Hegab S, Yataco AC, Tatem G, Salem D, Moore S, Boka K, et al. 2016 Early goal-directed therapy in severe sepsis and septic shock: insights and comparisons to ProCESS, ProMISe, and ARISE. Crit. Care 20: 160. [PubMed: 27364620]

5. Galley HF 2011 Oxidative stress and mitochondrial dysfunction in sepsis. Br. J. Anaesth. 107: 57–64. [PubMed: 21596843]

6. Warburg O 1956 On the origin of cancer cells. Science 123: 309–314. [PubMed: 13298683]

7. Bauerfeld CP, Rastogi R, Pirockinaite G, Lee I, Hüttemann M, Monks B, Birnbaum MJ, Franchi L, Nuñez G, and Samavati L. 2012 TLR4-mediated AKT activation is MyD88/TRIF dependent and critical for induction of oxidative phosphorylation and mitochondrial transcription factor A in murine macrophages. J. Immunol. 188: 2847–2857. [PubMed: 22312125]

8. Samavati L, Lee I, Mathes I, Lottspeich F, and Hüttemann M. 2008 Tumor necrosis factor alpha inhibits oxidative phosphorylation through tyrosine phosphorylation at subunit I of cytochrome c oxidase. J. Biol. Chem. 283: 21134–21144. [PubMed: 18534980]

9. Cheng S-C, Scicluna BP, Arts RJ, Gresnigt MS, Lachmandas E, Giamarellos-Bourboulis EJ, Kox M, Manjeri GR, Wagenaars JA, Cremer OL, et al. 2016 Broad defects in the energy metabolism of leukocytes underlie immunoparalysis in sepsis. Nat. Immunol. 17: 406–413. [PubMed: 26950237]

10. Wang X, Meng X, Kuhlman JR, Nelin LD, Nicol KK, English BK, and Liu Y. 2007 Knockout of Mkp-1 enhances the host inflammatory responses to gram-positive bacteria. J. Immunol. 178: 5312–5320. [PubMed: 17404316]

11. Wang X, Nelin LD, Kuhlman JR, Meng X, Welty SE, and Liu Y. 2008 The role of MAP kinase phosphatase-1 in the protective mechanism of dexamethasone against endotoxemia. Life Sci. 83: 671–680. [PubMed: 18845168]

12. Su J, Cui X, Li Y, Mani H, Ferreyra GA, Danner RL, Hsu LL, Fitz Y, and Eichacker PQ. 2010 SB203580, a p38 inhibitor, improved cardiac function but worsened lung injury and survival during *Escherichia coli* pneumonia in mice. J. Trauma 68: 1317–1327. [PubMed: 20068480]

13. Zhao Q, Shepherd EG, Manson ME, Nelin LD, Sorokin A, and Liu Y. 2005 The role of mitogen-activated protein kinase phosphatase-1 in the response of alveolar macrophages to lipopolysaccharide: attenuation of proinflammatory cytokine biosynthesis via feedback control of p38. J. Biol. Chem. 280: 8101–8108. [PubMed: 15590669]

14. Zhao Q, Wang X, Nelin LD, Yao Y, Matta R, Manson ME, Baliga RS, Meng X, Smith CV, Bauer JA, et al. 2006 MAP kinase phosphatase 1 controls innate immune responses and suppresses endotoxic shock. J. Exp. Med. 203: 131–140. [PubMed: 16380513]

15. Zhou X, Ferraris JD, Dmitrieva NI, Liu Y, and Burg MB. 2008 MKP-1 inhibits high NaCl-induced activation of p38 but does not inhibit the activation of TonEBP/OREBP: opposite roles of p38alpha and p38delta. Proc. Natl. Acad. Sci. USA 105: 5620–5625. [PubMed: 18367666]

16. Doi M, Cho S, Yujnovsky I, Hirayama J, Cermakian N, Cato AC, and Sassone-Corsi P. 2007 Light-inducible and clock-controlled expression of MAP kinase phosphatase 1 in mouse central pacemaker neurons. J. Biol. Rhythms 22: 127–139. [PubMed: 17440214]

17. Shipp LE, Lee JV, Yu CY, Pufall M, Zhang P, Scott DK, and Wang JC. 2010 Transcriptional regulation of human dual specificity protein phosphatase 1 (DUSP1) gene by glucocorticoids. PLoS One 5: e13754. [PubMed: 21060794]

18. Liu Y, Shepherd EG, and Nelin LD. 2007 MAPK phosphatases-regulating the immune response. Nat. Rev. Immunol. 7: 202–212. [PubMed: 17318231]

19. Liu YX, Wang J, Guo J, Wu J, Lieberman HB, and Yin Y. 2008 DUSP1 is controlled by p53 during the cellular response to oxidative stress. Mol. Cancer Res. 6: 624–633. [PubMed: 18403641]

20. Rastogi R, Du W, Ju D, Pirockinaite G, Liu Y, Nunez G, and Samavati L. 2011 Dysregulation of p38 and MKP-1 in response to NOD1/TLR4 stimulation in sarcoid bronchoalveolar cells. Am. J. Respir. Crit. Care Med. 183: 500–510. [PubMed: 20851927]

21. Frazier WJ, Wang X, Wancket LM, Li XA, Meng X, Nelin LD, Cato AC, and Liu Y. 2009 Increased inflammation, impaired bacterial clearance, and metabolic disruption after gram-negative sepsis in Mkp-1-deficient mice. J. Immunol. 183: 7411–7419. [PubMed: 19890037]
22. Lawan A, Min K, Zhang L, Canfran-Duque A, Jurczak MJ, Camporez JPG, Nie Y, Gavin TP, Shulman GI, Fernandez-Hernando C, and Bennett AM. 2018 Skeletal muscle-specific deletion of MKP-1 reveals a p38 MAPK/JNK/Akt signaling node that regulates obesity-induced insulin resistance. Diabetes 67: 624–635. [PubMed: 29317435]
23. Wang L, Waltenberger B, Pferschy-Wenzig E-M, Blunder M, Liu X, Malainer C, Blazevic T, Schwaiger S, Rollinger JM, Heiss EH, et al. 2014 Natural product agonists of peroxisome proliferator-activated receptor gamma (PPARg): a review. Biochem. Pharmacol. 92: 73–89. [PubMed: 25083916]
24. Roth RJ, Le AM, Zhang L, Kahn M, Samuel VT, Shulman GI, and Bennett AM. 2009 MAPK phosphatase-1 facilitates the loss of oxidative myofibers associated with obesity in mice. J. Clin. Invest. 119: 3817–3829. [PubMed: 19920356]
25. Talwar H, Bauerfeld C, Bouhamdan M, Farshi P, Liu Y, and Samavati L. 2017 MKP-1 negatively regulates LPS-mediated IL-1β production through p38 activation and HIF-1$\alpha$ expression. Cell. Signal. 34: 1–10. [PubMed: 28238855]
26. Talwar H, Bauerfeld C, Liu Y, and Samavati L. 2017 The dataset describes: HIF-1α expression and LPS mediated cytokine production in MKP-1 deficient bone marrow derived murine macrophages. Data Brief 14: 56–61. [PubMed: 28765831]
27. Maxwell PH, Wiesener MS, Chang G-W, Clifford SC, Vaux EC, Cockman ME, Wykoff CC, Pugh CW, Maher ER, and Ratcliffe PJ. 1999 The tumour suppressor protein VHL targets hypoxia-inducible factors for oxygen-dependent proteolysis. Nature 399: 271–275. [PubMed: 10353251]
28. Semenza GL 2003 Targeting HIF-1 for cancer therapy. Nat. Rev. Cancer 3: 721–732. [PubMed: 13130303]
29. Tannahill GM, Curtis AM, Adamik J, Palsson-McDermott EM, McGettrick AF, Goel G, Frezza C, Bernard NJ, Kelly B, Foley NH, et al. 2013 Succinate is an inflammatory signal that induces IL-1β through HIF-1$\alpha$. Nature 496: 238–242. [PubMed: 23535595]
30. Walmsley SR, Print C, Farahi N, Peyssonnaux C, Johnson RS, Cramer T, Sobolewski A, Condliffe AM, Cowburn AS, Johnson N, and Chilvers ER. 2005 Hypoxia-induced neutrophil survival is mediated by HIF-1$\alpha$-dependent NF-kappaB activity. J. Exp. Med. 201: 105–115. [PubMed: 15630139]
31. Talreja J, Talwar H, Ahmad N, Rastogi R, and Samavati L. 2016 Dual inhibition of Rip2 and IRAK1/4 regulates IL-1β and IL-6 in sarcoidosis alveolar acrophages and peripheral blood ononuclear cells. J. Immunol. 197: 1368–1378. [PubMed: 27402699]
32. Jornayvaz FR, and Shulman GI. 2010 Regulation of mitochondrial biogenesis. Essays Biochem. 47: 69–84. [PubMed: 20533901]
33. Talreja J, and Samavati L. 2018 K63-linked polyubiquitination on TRAF6 regulates LPS-mediated MAPK activation, cytokine production, and bacterial clearance in toll-like receptor 7/8 primed murine macrophages. Front. Immunol. 9: 279. [PubMed: 29515583]
34. Talwar H, Bouhamdan M, Bauerfeld C, Talreja J, Aoidi R, Houde N, Charron J, and Samavati L. 2019 MEK2 negatively regulates lipopolysaccharide-mediated IL-1β production through HIF-1$\alpha$ expression. J. Immunol. 202: 1815–1825. [PubMed: 30710049]
35. Li J, Wang X, Ackerman WE IV., Batty AJ, Kirk SG, White WM, Wang X, Anastasakis D, Samavati L, Buhimschi I, et al. 2018 Dysregulation of lipid metabolism in Mkp-1 deficient mice during gram-negative sepsis. Int. J. Mol. Sci. 19: 3904.
36. Rastogi R, Jiang Z, Ahmad N, Rosati R, Liu Y, Beuret L, Monks R, Charron J, Birnbaum MJ, and Samavati L. 2013 Rapamycin induces mitogen-activated protein (MAP) kinase phosphatase-1 (MKP-1) expression through activation of protein kinase B and mitogen-activated protein kinase kinase pathways. J. Biol. Chem. 288: 33966–33977. [PubMed: 24126911]
37. Papathanassiu AE, Ko J-H, Imprialou M, Bagnati M, Srivastava PK, Vu HA, Cucchi D, McAdoo SP, Ananieva EA, Mauro C, and Behmoaras J. 2017 BCAT1 controls metabolic reprogramming in activated human macrophages and is associated with inflammatory diseases. Nat. Commun. 8: 16040. [PubMed: 28699638]

38. Chi H, Barry SP, Roth RJ, Wu JJ, Jones EA, Bennett AM, and Flavell RA. 2006 Dynamic regulation of pro- and anti-inflammatory cytokines by MAPK phosphatase 1 (MKP-1) in innate immune responses. Proc. Natl. Acad. Sci. USA 103: 2274–2279. [PubMed: 16461893]
39. Raman M, Chen W, and Cobb MH. 2007 Differential regulation and properties of MAPKs. Oncogene 26: 3100–3112. [PubMed: 17496909]
40. Kelly B, and O'Neill LA. 2015 Metabolic reprogramming in macrophages and dendritic cells in innate immunity. Cell Res. 25: 771–784. [PubMed: 26045163]
41. Sinclair LV, Rolf J, Emslie E, Shi Y-B, Taylor PM, and Cantrell DA. 2013 Control of amino-acid transport by antigen receptors coordinates the metabolic reprogramming essential for T cell differentiation. [Published erratum appears in 2014 Nat. Immunol. 15: 109.] Nat. Immunol. 14: 500–508. [PubMed: 23525088]
42. Culotta VC, Yang M, and O'Halloran TV. 2006 Activation of superoxide dismutases: putting the metal to the pedal. Biochim. Biophys. Acta 1763: 747–758. [PubMed: 16828895]
43. Tainer JA, Getzoff ED, Richardson JS, and Richardson DC. 1983 Structure and mechanism of copper, zinc superoxide dismutase. Nature 306: 284–287. [PubMed: 6316150]
44. Ngo HB, Lovely GA, Phillips R, and Chan DC. 2014 Distinct structural features of TFAM drive mitochondrial DNA packaging versus transcriptional activation. Nat. Commun. 5: 3077. [PubMed: 24435062]
45. Scarpulla RC 2008 Transcriptional paradigms in mammalian mitochondrial biogenesis and function. Physiol. Rev. 88: 611–638. [PubMed: 18391175]
46. Rao SP, Alonso S, Rand L, Dick T, and Pethe K. 2008 The protonmotive force is required for maintaining ATP homeostasis and viability of hypoxic, nonreplicating *Mycobacterium tuberculosis*. Proc. Natl. Acad. Sci. USA 105: 11945–11950. [PubMed: 18697942]
47. Rutter J, Winge DR, and Schiffman JD. 2010 Succinate dehydrogenase assembly, regulation and role in human disease. Mitochondrion 10: 393–401. [PubMed: 20226277]
48. Zhou J-Y, Liu Y, and Wu GS. 2006 The role of mitogen-activated protein kinase phosphatase-1 in oxidative damage-induced cell death. Cancer Res. 66: 4888–4894. [PubMed: 16651445]
49. Flynn JM, and Melov S. 2013 SOD2 in mitochondrial dysfunction and neurodegeneration. Free Radic. Biol. Med. 62: 4–12. [PubMed: 23727323]
50. Rogers RJ, Monnier JM, and Nick HS. 2001 Tumor necrosis factor-alpha selectively induces MnSOD expression via mitochondriato-nucleus signaling, whereas interleukin-1beta utilizes an alternative pathway. J. Biol. Chem. 276: 20419–20427. [PubMed: 11264281]
51. Tsan MF, Clark RN, Goyert SM, and White JE. 2001 Induction of TNF-alpha and MnSOD by endotoxin: role of membrane CD14 and toll-like receptor-4. Am. J. Physiol. Cell Physiol. 280: C1422–C1430. [PubMed: 11350737]
52. Wang Y, Branicky R, Noë A, and Hekimi S. 2018 Superoxide dismutases: dual roles in controlling ROS damage and regulating ROS signaling. J. Cell Biol. 217: 1915–1928. [PubMed: 29669742]
53. Fukuzumi M, Shinomiya H, Shimizu Y, Ohishi K, and Utsumi S. 1996 Endotoxin-induced enhancement of glucose influx into murine peritoneal macrophages via GLUT1. Infect. Immun. 64: 108–112. [PubMed: 8557327]
54. Goda N, and Kanai M. 2012 Hypoxia-inducible factors and their roles in energy metabolism. Int. J. Hematol. 95: 457–463. [PubMed: 22535382]
55. Minchenko A, Leshchinsky I, Opentanova I, Sang N, Srinivas V, Armstead V, and Caro J. 2002 Hypoxia-inducible factor-1-mediated expression of the 6-phosphofructo-2-kinase/fructose-2,6-bisphosphatase-3 (PFKFB3) gene. Its possible role in the Warburg effect. J. Biol. Chem. 277: 6183–6187. [PubMed: 11744734]
56. Michelucci A, Cordes T, Ghelfi J, Pailot A, Reiling N, Gold-mann O, Binz T, Wegner A, Tallam A, Rausell A, et al. 2013 Immune-responsive gene 1 protein links metabolism to immunity by catalyzing itaconic acid production. Proc. Natl. Acad. Sci. USA 110: 7820–7825. [PubMed: 23610393]
57. O'Neill LA, and Pearce EJ. 2016 Immunometabolism governs dendritic cell and macrophage function. J. Exp. Med. 213: 15–23. [PubMed: 26694970]

58. Wu JJ, Roth RJ, Anderson EJ, Hong E-G, Lee M-K, Choi CS, Neufer PD, Shulman GI, Kim JK, and Bennett AM. 2006 Mice lacking MAP kinase phosphatase-1 have enhanced MAP kinase activity and resistance to diet-induced obesity. Cell Metab. 4: 61–73. [PubMed: 16814733]

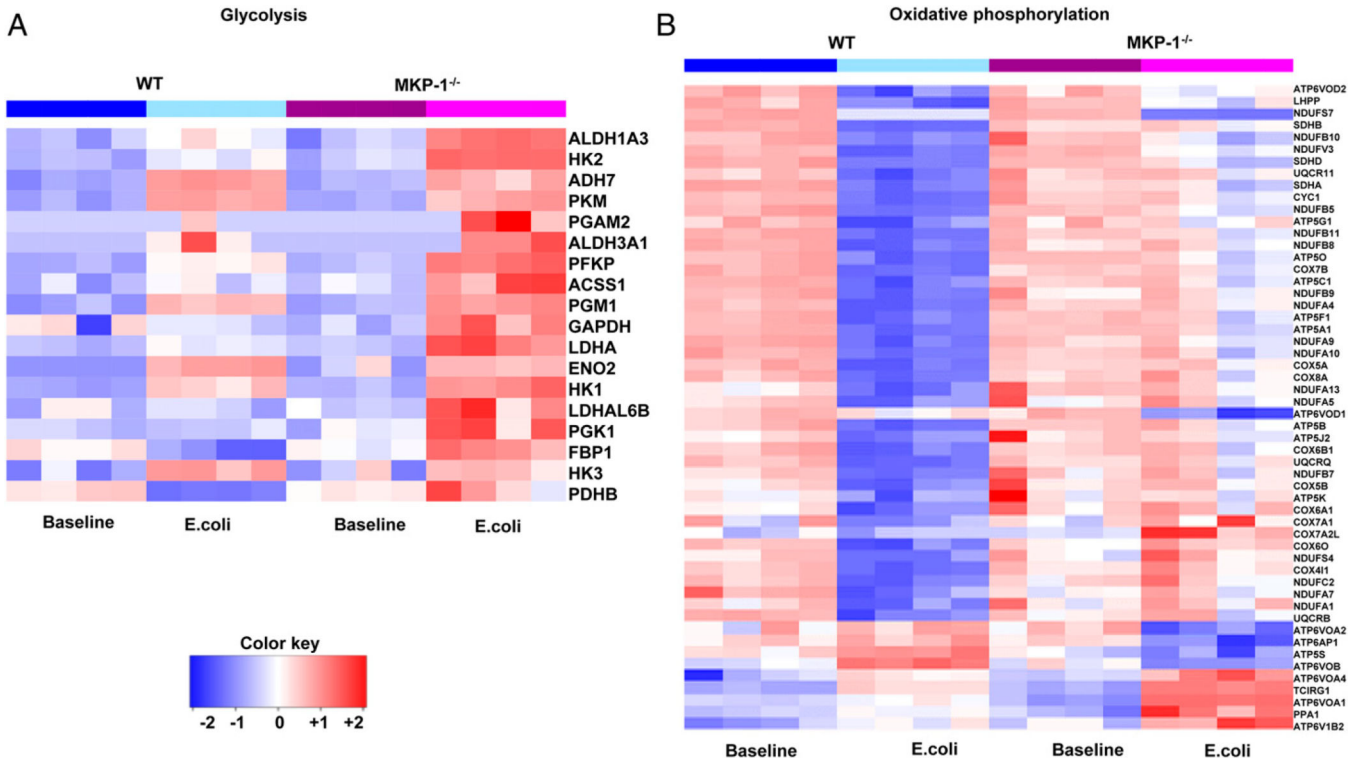


**FIGURE 1. Livers of MKP-1$^{-/-}$ mice exhibit aberrant expression profiles for genes involved in glycolysis and OxPhos.**

WT mice respond to *E. coli* sepsis with an increased expression of glycolysis genes, decreased expression for OxPhos genes. In contrast, MKP-1$^{-/-}$ mice show upregulation of glycolysis but dysregulated OxPhos. (**A**) Major genes involved in glycolysis. (**B**) Selected genes involved in OxPhos. Data represent four animals in each group.

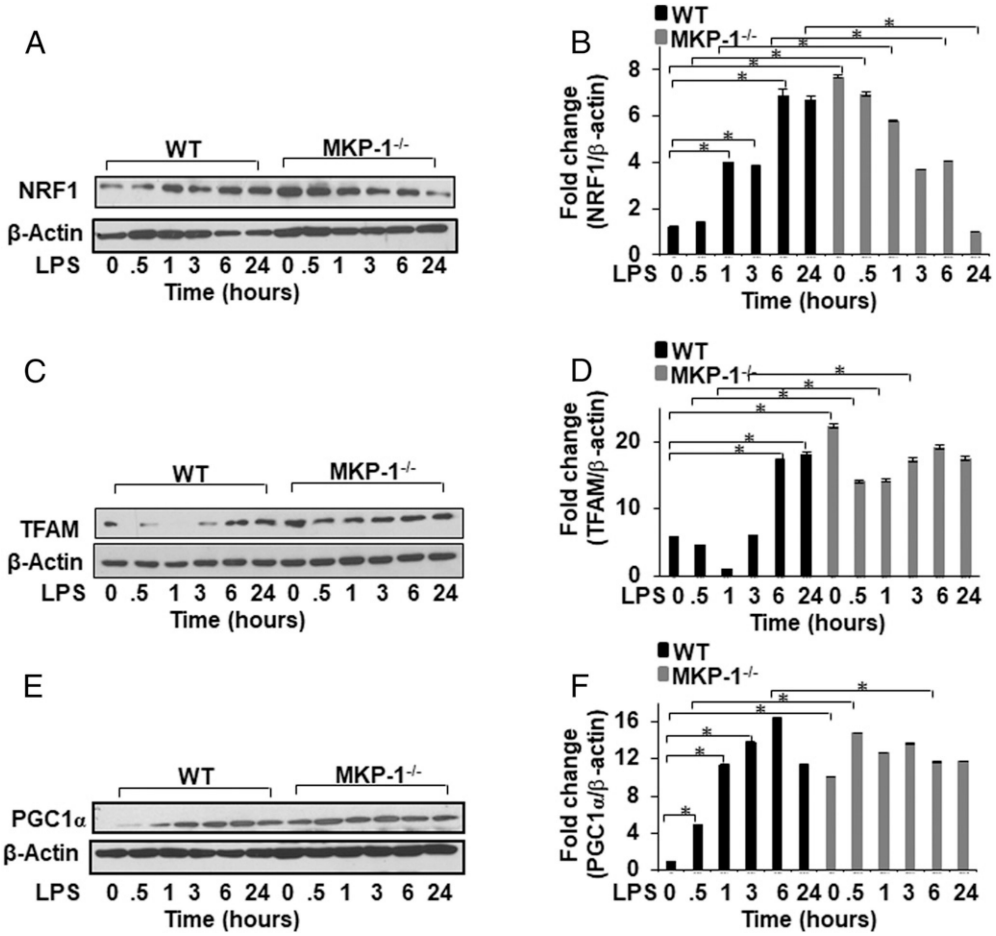


**FIGURE 2. Increased protein levels of mitochondrial transcription factors (NRF-1, TFAM, and PGC-1*α*) in MKP-1$^{-/-}$ BMDMs as compared with WT BMDMs.**

BMDMs derived from WT and MKP-1$^{-/-}$ were cultured and treated with LPS (100 ng/ml) for 30 min and 1, 3, 6, and 24 h. Whole-cell extracts were prepared and subjected to Western blot analysis using specific Abs against NRF-1 (**A**), TFAM (**C**), and PGC-1*α* (**E**). Equal loading was performed using β-actin. Densitometric values expressed as fold changes of the ratio of NRF-1/β-actin (**B**), TFAM/β-actin (**D**), and PGC-1*α*/β-actin (**F**). As shown, MKP-1$^{-/-}$ BMDMs exhibited a significant increase in protein levels of all the transcription factors at basal levels. In contrast, in response to LPS treatment WT BMDMs responded with a time-dependent increase in NRF-1, TFAM, and PGC-1*α* protein level, whereas MKP-1–deficient macrophages failed to do so. Data represent mean ± SEM of at least four independent experiments. *$p < 0.05$.

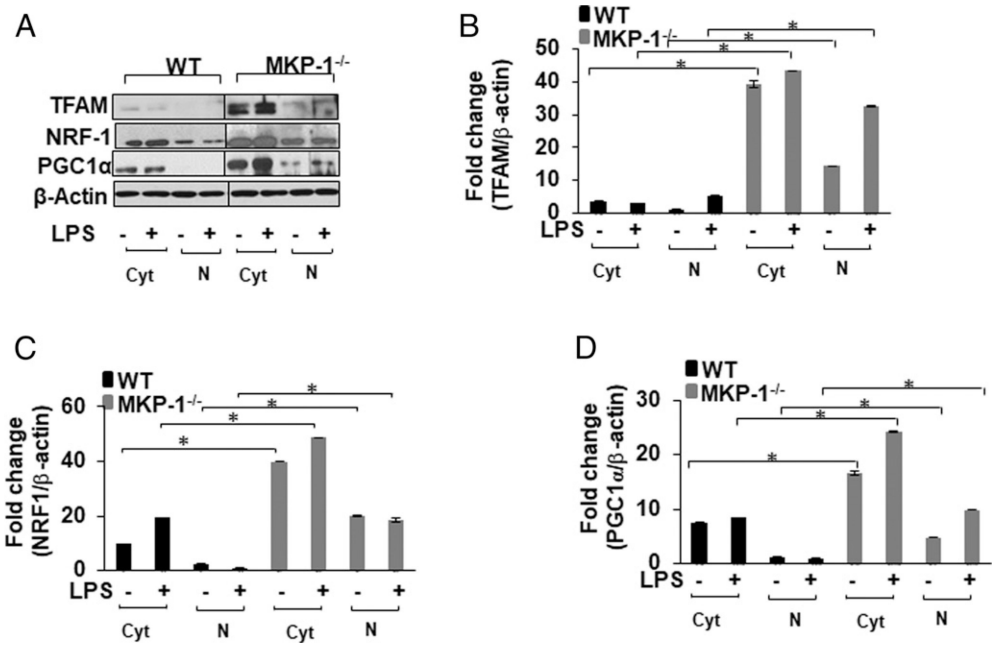


**FIGURE 3. MKP-1$^{-/-}$ BMDMs exhibit increased protein levels of mitochondrial transcription factors (TFAM, NRF-1, and PGC-1$\alpha$) in cytosolic and nuclear fractions.**

WT and MKP-1–deficient macrophages were cultured under similar conditions and challenged with LPS (100 ng/ml) for 3 h. Cytosolic and nuclear extracts were prepared and subjected to SDS-PAGE. Western blot analyses were performed using specific Abs to TFAM, NRF-1, and PGC-1$\alpha$ transcription factors. Equal loading was confirmed with β-actin (**A**). Densitometric values expressed as fold changes of the ratio of NRF-1/β-actin (**B**), TFAM/β-actin (**C**), and PGC-1$\alpha$/β-actin (**D**). MKP-1 deficient macrophages exhibited marked increase in protein levels of all three transcription factors in cytosolic and nuclear fractions at baseline and in response to LPS challenge. Data represent mean ± SEM of at least four independent experiments. *$p < 0.05$.

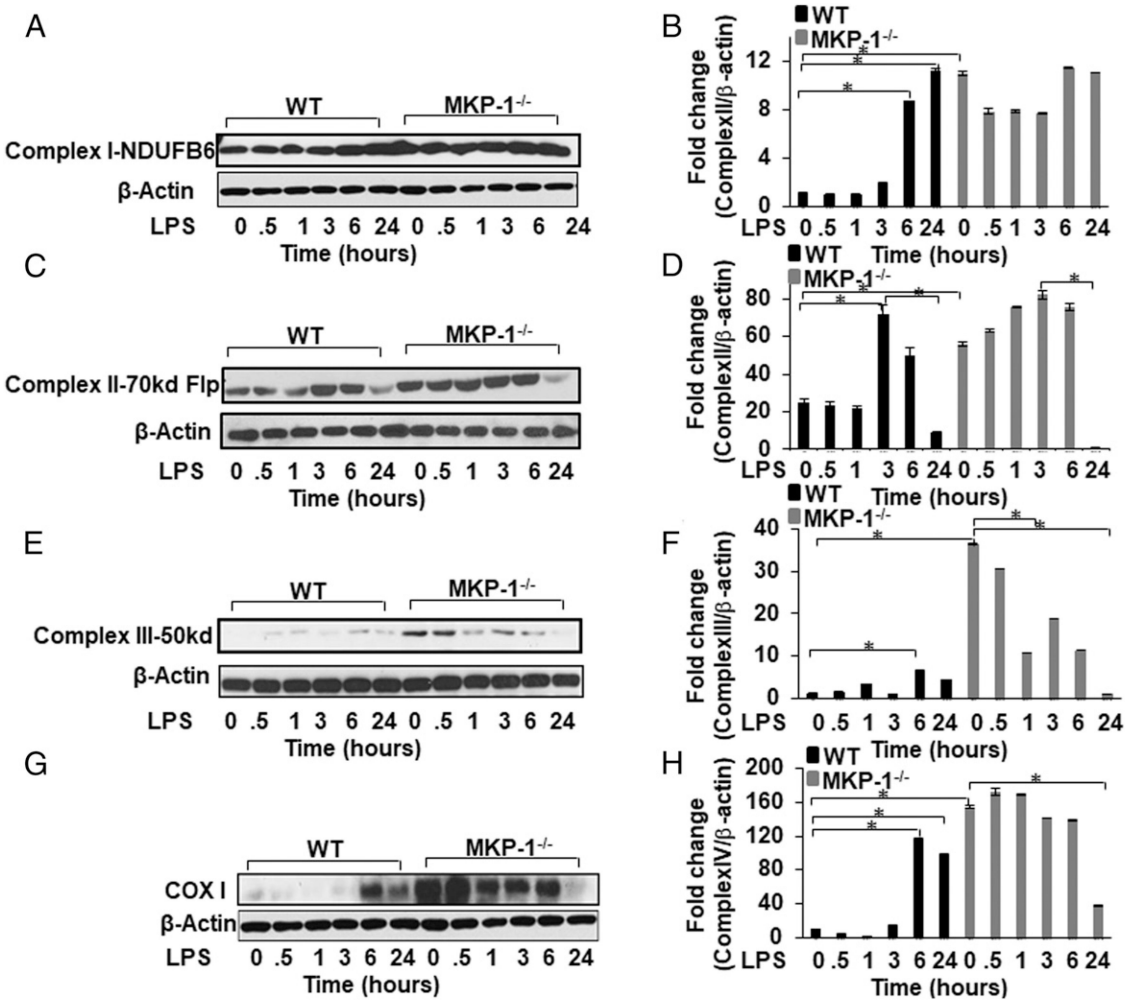


**FIGURE 4. Higher protein levels of OxPhos complexes in MKP-1$^{-/-}$ BMDMs as compared with WT BMDMs.**

WT and MKP-1$^{-/-}$ BMDMs were treated with LPS (100 ng/ml) for 30 min and 1, 3, 6, and 24 h. Whole-cell extracts were prepared and Western blot analysis performed using specific Abs against complex I NADH: ubiquinone oxidoreductase subunit 6 (NDUFB6) (**A**), Complex II succinate dehydrogenase–70 kDa Flp (**C**), complex III- ubiquinol: cytochrome *c* oxidoreductase–50 kDa (**E**), and complex IV–COXI (**G**). Equal loading was confirmed using Ab against β-actin. Densitometric values expressed as fold changes of the ratio of the corresponding complexes (I-IV)/β-actin (**B**, **D**, **F**, and **H**). As shown, MKP-1$^{-/-}$ BMDMs exhibited increased protein levels of all the complexes at baseline as compared with WT BMDMs. In response to LPS, WT BMDMs showed an increased induction of OxPhos. In contrast, MKP-1$^{-/-}$ BMDMs show no significant upregulation (complex I NDUFB6) or a decrease in protein expression for complexes II–IV as compared with WT BMDMs. Data represent mean ± SEM of at least four independent experiments. *$p < 0.05$.

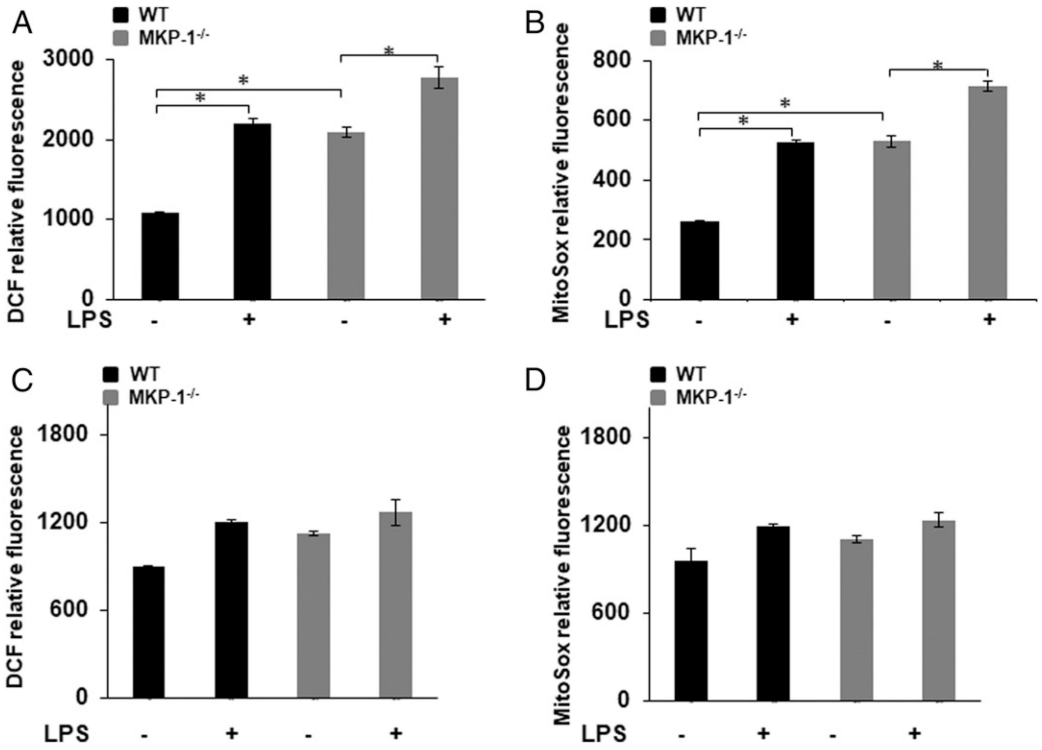


**FIGURE 5. MKP-1$^{-/-}$ BMDMs exhibit higher ROS production as compared with WT BMDMs.**
WT and MKP-1$^{-/-}$ BMDMs were treated with and without LPS (100 ng/ml) for 1 and 24 h, followed by measurement of ROS production using H2DCFDA and MitoSOX fluorescence intensity. Basal ROS production is significantly higher in MKP-1$^{-/-}$ BMDMs compared with WT BMDMs. LPS challenge for 1 h induced ROS production both in WT and MKP-1$^{-/-}$ BMDMs (**A** and **B**). ROS production at baseline and after LPS challenge for 24 h is not significantly different between WT and MKP-1$^{-/-}$ BMDMs (**C** and **D**). Data represent mean ± SEM of three independent experiments. *$p < 0.05$.

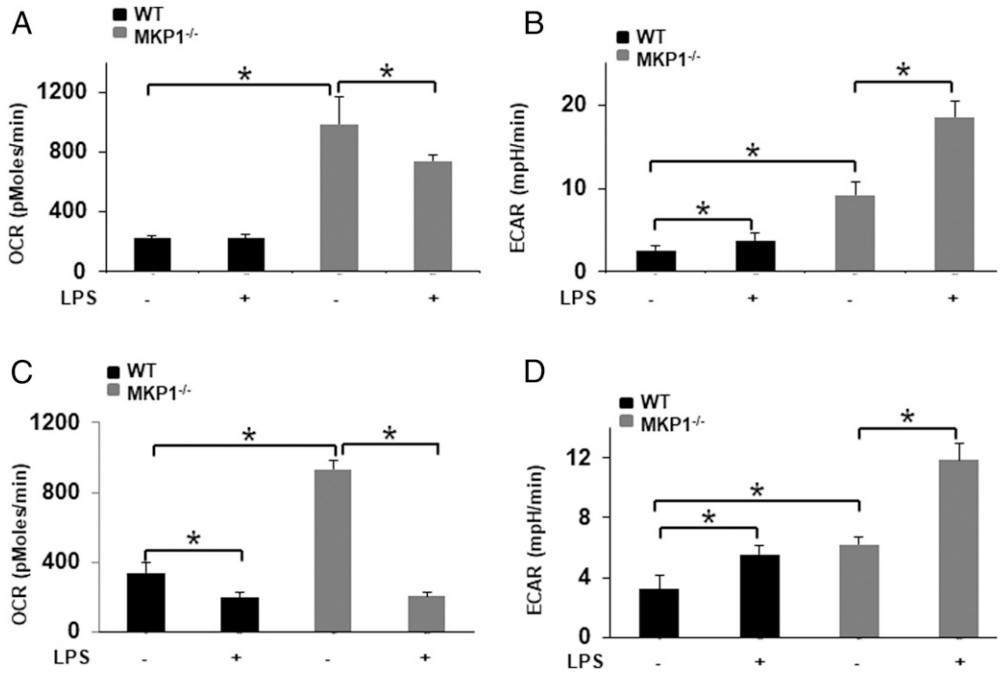


**FIGURE 6. MKP-1–deficient BMDMs exhibit higher OCR and ECAR as compared with WT BMDMs. Basal OCR and ECAR were measured on a Seahorse XF$^{e}$ bioanalyzer.**

WT and MKP-1$^{-/-}$ BMDMs were treated with vehicle or LPS (100 ng/ml) for 3 h, followed by measurement of OCR and ECAR expressed per 100,000 cells in picomoles per minute and milli-pH per minute (**A** and **B**). Basal OCR and acidification rate are increased in MKP-1$^{-/-}$ BMDMs. LPS treatment resulted in significant decrease in OCR in MKP-1$^{-/-}$ BMDMs as compared with WT BMDMs. In contrast, LPS-induced ECAR significantly increased in both WT and MKP-1$^{-/-}$ BMDMs (A and B). Additionally, LPS (100 ng/ml) for 24 h decreased OCR and increased ECAR significantly in both WT and MKP-1$^{-/-}$ BMDMs (**C** and **D**). Data represent mean ± SEM of six independent experiments. *$p < 0.05$.

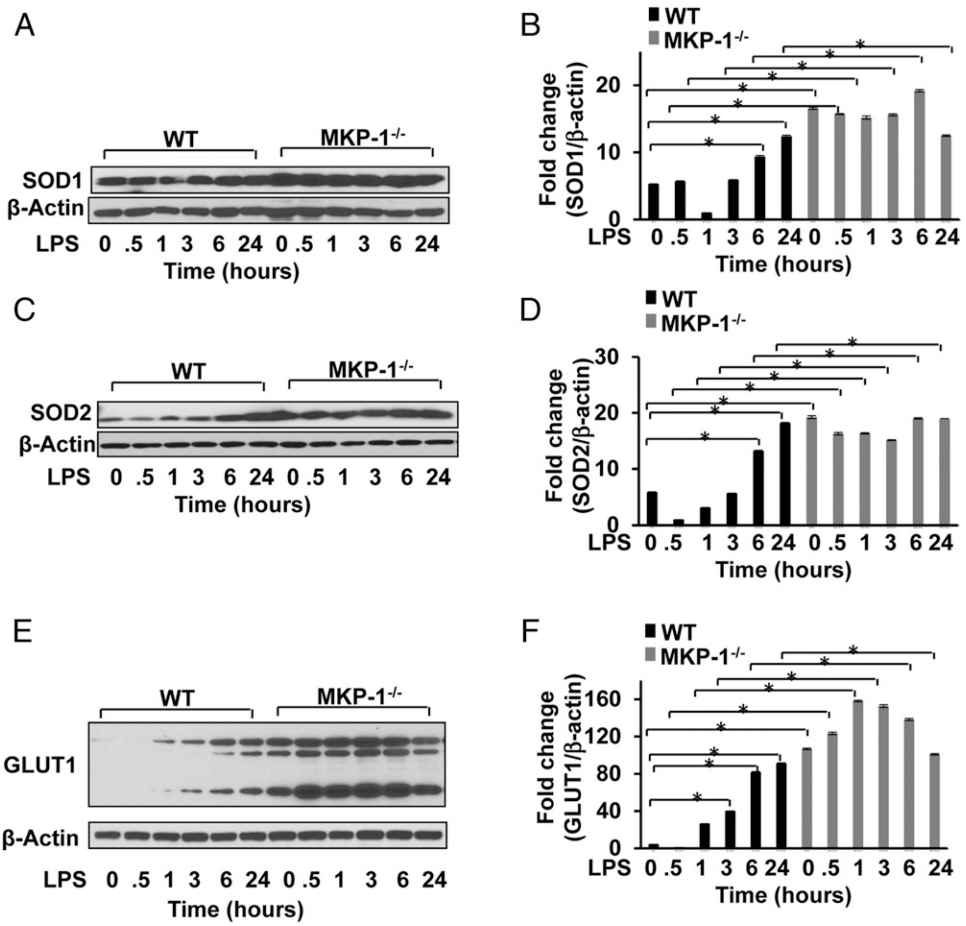


**FIGURE 7. MKP-1$^{-/-}$ BMDMs exhibit higher SOD1 and SOD2 protein levels in response to LPS.**

BMDMs derived from WT and MKP-1$^{-/-}$ mice were cultured and treated with LPS (100 ng/ml) for 30 min and 1, 3, 6, and 24 h. Whole-cell extracts were prepared and subjected to Western blot analysis using specific Abs against SOD1 and SOD2. Equal loading was confirmed using Ab against β-actin. As shown, MKP-1$^{-/-}$ BMDMs exhibited higher protein levels of SOD1 and SOD2 both at baseline and in response to LPS (**A** and **C**). Densitometric values expressed as fold changes of the ratio of SOD1/β-actin and SOD2/β-actin (**B** and **D**). WT and MKP-1 deficient BMDMs were treated with LPS (100 ng/ml) for 30 min and 1, 3, 6, and 24 h. Whole-cell extracts were subjected to immunoblotting using Abs against GLUT1 and β-actin (**E**). Densitometric values are expressed as fold changes of the ratio of GLUT1/β-actin (**F**). Data represent mean ± SEM of at least three independent experiments. *$p < 0.05$.

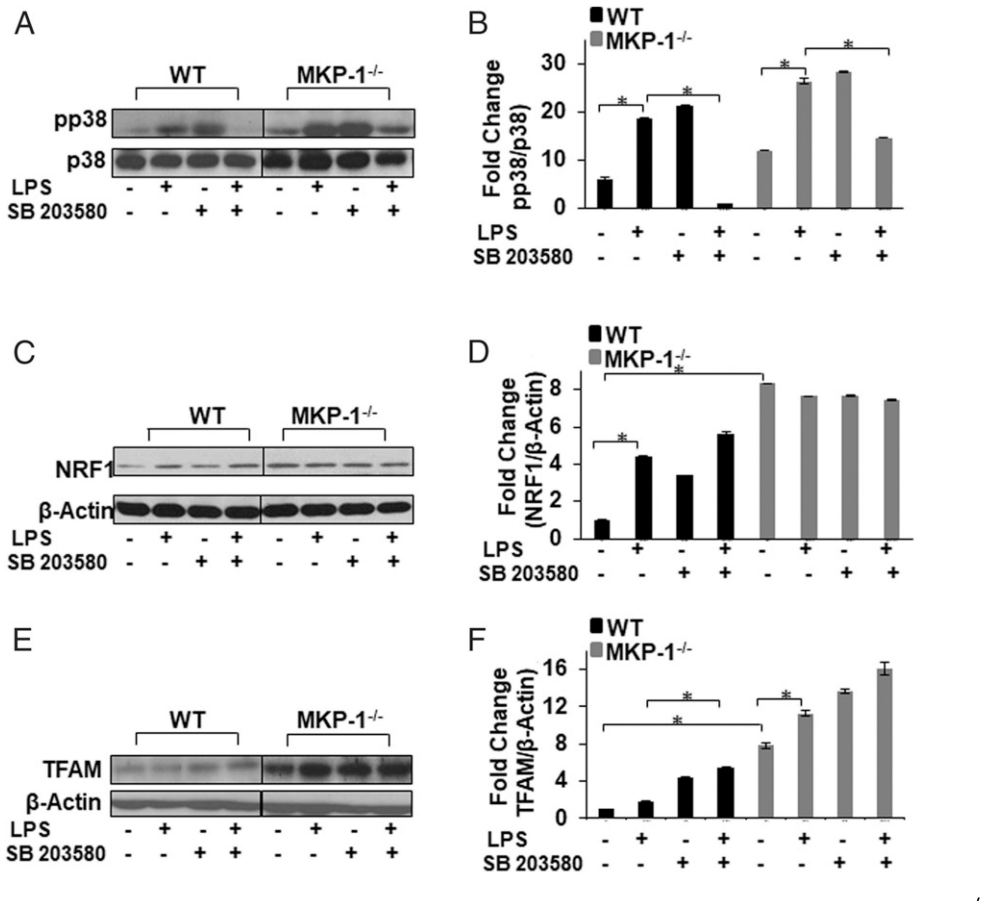


**FIGURE 8. Inhibitor of p38 MAP kinase has no effect on LPS-mediated NRF-1 and TFAM protein levels in WT and MKP-1$^{-/-}$ BMDMs.**

BMDMs derived from WT and MKP-1–deficient mice were cultured in the presence and absence of SB203850 (10 μM), followed by a challenge with LPS for 3 h. Western blot analysis was performed using phospho-specific Ab against p38 (Thr$^{180}$/Tyr$^{182}$) and equal loading was confirmed with total p38 Ab (**A**). Densitometric values expressed as fold increase of the ratio of pp38/p38 ($n = 3$) (**B**). Western blot analysis was performed using specific Ab against NRF-1 (**C**). Densitometric values expressed as fold increase of the ratio of NRF-1/β-actin ($n = 3$) (**D**). Western blot analysis was performed using specific Ab against TFAM (**E**). Densitometric values expressed as fold increase of the ratio of TFAM/β-actin ($n = 3$) (**F**). Results indicate that pretreatment with SB203850 had no effect on the LPS-induced NRF-1 or TFAM transcription factors. Data represent mean ± SEM of three independent experiments. *$p < 0.05$.